Available online at www.sciencedirect.com
ScienceDirect
Biochimica et Biophysica Acta 1778 (2008) 324–333
Biochimica et Biophysica Acta
BBA
www.elsevier.com/locate/bbamem

Structural stability of GlcV, the nucleotide binding domain of the glucose ABC transporter of *Sulfolobus solfataricus*

Monika G. Pretz [a,1], Chris van der Does [a], Sonja-Verena Albers [a], Gea Schuurman-Wolters [b], Arnold J.M. Driessen [a,*]

[a] *Department of Molecular Microbiology, Groningen Biomolecular Sciences and Biotechnology Institute and Zernike Institute of Advanced Materials, University of Groningen, Kerklaan 30, 9751 NN Haren, The Netherlands*
[b] *Department of Biochemistry, Groningen Biomolecular Sciences and Biotechnology Institute, University of Groningen, Nijenborgh 4, 9727 AG Groningen, The Netherlands*

Received 24 August 2007; received in revised form 1 October 2007; accepted 5 October 2007
Available online 13 October 2007

Abstract

GlcV is the nucleotide binding domain of the ABC-type glucose transporter of the hyperthermoacidophile *Sulfolobus solfataricus*. GlcV consists of two domains, an N-terminal domain containing the typical nucleotide binding-fold and a C-terminal β-barrel domain with unknown function. The unfolding and structural stability of the wild-type (wt) protein and three mutants that are blocked at different steps in the ATP hydrolytic cycle were studied. The G144A mutant is unable to dimerize, while the E166A and E166Q mutants are defective in ATP hydrolysis and dimer dissociation. Unfolding of the wt GlcV and G144A GlcV occurred with a single transition, whereas the E166A and E166Q mutants showed a second transition at a higher melting temperature indicating an increased stability of the ABCα/β subdomain. The structural stability of GlcV was increased in the presence of nucleotides suggesting that the transition corresponds to the unfolding of the NBD domain. Unfolding of the C-terminal domain appears to occur at temperatures above the unfolding of the NBD which coincides with the aggregation of the protein. Analysis of the domain organization of GlcV by trypsin digestion demonstrates cleavage of the NBD domain into three fragments, while nucleotides protect against proteolysis. The cleaved GlcV protein retained the ability to bind nucleotides and to dimerize. These data indicate that the wt GlcV NBD domain unfolds as a single domain protein, and that its stability is modified by mutations in the glutamate after the Walker B motif and by nucleotide binding.
© 2007 Elsevier B.V. All rights reserved.

Keywords: ABC transporters; Nucleotide binding; Differential scanning calorimetry; Protein unfolding; Dimerization

1. Introduction

ATP binding cassette (ABC) transporters drive the transport of substrates across the membrane by the hydrolysis of ATP [1,2]. ABC transporters have a conserved domain structure, with two membrane-spanning domains that form the transport channel and two cytosolic nucleotide binding domains (NBDs) that energize the transport via the hydrolysis of ATP. The NBD is the most conserved domain of ABC transporters, and it comprises a number of highly conserved amino acid sequences that are involved in the binding and hydrolysis of nucleotides such as the Walker A and B motifs [3], the Q-, D- [4], H-loops [5] and A-loop [6] and the ABC signature motif [7,8]. The crystal structures of the NBDs of isolated NBDs [9–20] and complete ABC transporters [21–25] showed a typical fold which consists of two subdomains, named ABCα/β and ABCα, respectively. The ABCα/β subdomain consists of central β-sheets which are flanked by α-helices. This subdomain contains the Walker A and B motifs and is found also in proteins involved in cellular functions such as double strand DNA repair (Rad50) [4], DNA

Abbreviations: ABC, ATP binding cassette; DSC, differential scanning calorimetry; GdnCl, Guandiniumchloride; NBD, nucleotide binding domain; wt, wild-type; AMP-PNP, adenosine-(β,γ-imido)triphosphate

* Corresponding author. Tel.: +31 50 3632150; fax: +31 50 3632154.
E-mail address: a.j.m.driessen@rug.nl (A.J.M. Driessen).
[1] Present address: Hungarian Academy of Science, Institute of Enzymology 1113, Budapest, Karolina ut 29, Hungary.

0005-2736/$ - see front matter © 2007 Elsevier B.V. All rights reserved.
doi:10.1016/j.bbamem.2007.10.004

mismatch repair (MutS) [26] chromosome condensation (SMC) [27] and ribosome biogenesis (RLI) [28]. The ABCα subdomain is an insertion of 70 residues between the β6 and β7 strands of the ABCα/β subdomain, and contains mainly α-helices and the highly conserved ABC signature motif and Q-loop. While the Walker A and B motifs are common for P-loop nucleotide triphosphate binding proteins and involved in the coordination of ATP and Mg^{2+}, the Q-, D- and H-loops and ABC signature motifs are unique features of ABC ATPases [2,29]. The highly conserved residues of the C-loop motif participate in the binding and hydrolysis of ATP and mutants thereof were defective in ATP hydrolysis while retaining the ability to bind ATP. Mutagenesis of the glutamine, the histidine and the aspartate in the Q-, H- and D-loops, respectively, results in defective transport.

Crystal structures of the monomeric NBDs showed that the C-loop motif is far away from the nucleotide binding domain. On the other hand, the structure of the ATPase domain of Rad50 in complex with ATP showed a head-to-tail organization of two monomers [4]. In this dimer, the nucleotide is sandwiched between the Walker A and B domains of one monomer and ABC signature motif of the other monomer. Such ATP-induced dimerization was further demonstrated for several NBDs of ABC transporters which formed a stable ATP-induced NBD dimer after mutation of the putative catalytic glutamate adjacent to the Walker B motif [13,30,31], for wild-type *Escherichia coli* MalK [32], and HlyB with a mutation in the histidine of the H-loop [15]. Dimerization of GlcV was indeed also observed after mutation of the glutamate adjacent to the Walker B motif [33,34]. A similar geometry of the ABC domains is observed in the structures of complete ABC transporters, although the nucleotide-free structures showed some separation of the two NBDs [22,24,25]. For the full length transporter, it has been proposed that the nucleotide induced dimerization of the NBDs drives a conformational change in the transmembrane domains leading to transport of the substrate [30,31,35–39].

Sequence alignment of bacterial and archaeal ABC ATPases revealed that the NBDs of some of these transporters harbor an additional C-terminal extension of about 130 residues. This extension is also found in many binding protein-dependent ABC transporters that mediate the uptake of solutes like maltose or glucose. The C-terminal extension of the MalK NBDs of the *E. coli* and *S. typhimurium* maltose transporters interacts with MalT, a transcriptional activator of the *mal* operon [40]. In the absence of maltose, MalT binds to MalK, whereas in the presence of maltose, MalT is released whereupon it activates transcription of the *mal* operon.

Sequence alignment (25% of sequence identity) and crystal structure comparison indicates that GlcV, the ABC ATPase of the glucose transporter from *Sulfolobus solfataricus* [13], has a similar domain organization as MalK of *E. coli* [17] and *Thermococcus litoralis* [10]. The N-terminal domain of GlcV consists of about 225 residues with a typical fold of ABC ATPases. The protein contains an additional 125 residues at its C-terminus, forming a β-barrel shaped structure very similar to the regulatory domain of *T. litoralis*. However, the additional α-helix in between β13 and β14 of the *E. coli* and *T. litoralis* β-barrel, is replaced by a loop region only in GlcV. The structural similarity also involves the linker region between the N- and C-terminal domains. Despite the high structural and sequence similarity between the C-terminal domain of MalK and GlcV, a regulatory function of this region in the *S. solfataricus* GlcV remains to be shown.

To further investigate the structural aspects of GlcV and its interaction with nucleotides, we have employed differential scanning calorimetry to study the unfolding of the isolated ABC ATPase. In this study, we compared the unfolding characteristics of the wild-type enzyme with that of two mutants that are defective in ATP hydrolysis. The data demonstrate that the NBD domain of GlcV thermodynamically behaves like a single domain protein that is stabilized by nucleotides.

2. Materials and methods

2.1. Cloning, expression and purification

Wild-type *S. solfataricus* GlcV and the G144A, E166A, and E166Q mutants were expressed using the pET2150, pET2183, pET2187 and pET2186 plasmids as described by Verdon et al [34]. Expression and purification was performed as described previously [41].

2.2. Differential scanning calorimetry

Purified GlcV was dialyzed against 20 mM MES pH 6.5 and 100 mM NaCl in the presence of 5 mM $MgCl_2$ or 2 mM EDTA. The pH of the buffer slightly decreased from pH 6.5 to 6.2 when the temperature was raised from 20 to 60 °C. Protein concentrations were determined spectrophotometrically using an extinction coefficient of 20,000 M^{-1} cm^{-1}, and were confirmed by determination of the protein concentration after total amino acid analysis (Eurosequence). DSC experiments were performed on a VP DSC (Microcal) using a differential scanning rate of 1 °C/min and a protein concentration of 30 μM. Similar experiments were performed at a scanning rate of 0.2 to 2 °C/min, but no significant differences were observed. Nucleotide stock solution (ATP, ADP or AMP-PNP) of 100 mM was adjusted to pH 6.5 with NaOH and diluted in dialysis buffer. The nucleotide concentration was determined spectroscopically using an extinction coefficient of 14,900 M^{-1} cm^{-1}. Where indicated, the nucleotide was added to the sample at a concentration of 600 μM either under hydrolyzing (5 mM $MgCl_2$) or non-hydrolyzing (2 mM EDTA) conditions. Before use, all solutions were degassed by gentle stirring under vacuum. The thermogram corresponding to the buffer was used as an instrumental baseline. The dependence of the molar heat capacity on temperature was analyzed using the Origin software 5.0 (Microcal). The experiments were performed in triplicate and the error in determination of the T_m was less than 0.3 °C. The reversibility of the DSC transitions was determined by termination of the DSC scan before the precipitation temperature and by re-heating of the solution in the calorimetric cell after cooling (1 °C/min).

2.3. Tryptophan fluorescence

Tryptophan emission spectra of wt GlcV (30 μM) were collected at room temperature in 20 mM MES pH 6.5, 100 mM NaCl, 5 mM $MgCl_2$ and increasing [0–6 M] Guanidiniumchloride (GdnCl) concentrations on a SLM Aminco–Bowman series 2 luminescence spectrometer at an excitation wavelength of 295 nm with a 5 nm bandwidth. Tryptophan emission spectra were recorded from 310 to 400 nm at a rate of 1 nm/s. When indicated, 1 mM ATP or ADP was added.

2.4. Trypsin cleavage assay

Purified wt and mutant GlcV (50 μg) was diluted in 50 μl buffer containing 20 mM MES pH 6.5, 100 mM NaCl and 5 mM $MgCl_2$ (binding buffer) at 20 °C.

After 1 min, 16 μg trypsin was added and the incubation was continued for 1 h. Reactions were stopped by the addition of 16 μg trypsin inhibitor (Lyophilized Soybean trypsin inhibitor (Type I-S) obtained from Sigma) from a 1 mg/ml stock solution, samples were mixed with SDS sample buffer and 10% was loaded on 15% SDS gel.

For nucleotide induced enzyme stability studies purified wt and mutant GlcV (50 μg) was pre-incubated in the absence or presence of 0.5 mM nucleotides (ATP, ADP and AMP-PNP) in 50 μl buffer containing 20 mM MES pH 6.5, 100 mM NaCl and 5 mM $MgCl_2$ (binding buffer) at 20 °C. After 5 min, 16 μg trypsin was added and the incubation was continued for 1 h. Again reactions were stopped by the addition of 16 μg trypsin inhibitor, and samples were mixed with SDS sample buffer and 10% was loaded on 15% SDS gel.

Nucleotide binding to trypsin digested GlcV was assayed by 8-Azido-ATP photoaffinity labelling. GlcV (0.3 μM) was incubated with 0.5 μM 8-azido-[α-^{32}P] ATP in binding buffer at 20 °C. After 5 min, samples were irradiated by UV (254 nm) for 2 min. Nucleotide bound GlcV was digested by the addition of 0.3 μM trypsin. After 30 min, 0.3 μM trypsin inhibitor was added and the protein was analyzed by SDS-PAGE and visualized by phosphor imaging. In another experiment, GlcV (0.3 μM) was first incubated with 0.3 μM trypsin prior to the photoaffinity labelling.

2.5. Size-exclusion chromatography

To remove residual uncleaved GlcV, red agarose purified samples were applied to Superdex 75 PC 16/60 gel filtration column. The column was equilibrated with 20 mM MES pH 6.5, 100 mM NaCl and 5 mM $MgCl_2$ and eluted with a similar buffer with 1 M NaCl. Protein elution was monitored at 254 and 280 nm. Trypsin and trypsin inhibitor were only detected in the non-bound fraction of the red agarose column. Samples were analyzed by 15% SDS-PAGE and coomassie brilliant blue staining.

2.6. Mass spectrometry

Bands were isolated from the SDS-PAGE gel, and the pieces of gel were fragmented in smaller pieces, destained in 50 mM ammonium bicarbonate in 40% ethanol, dehydrated by a three times repeated treatment with 100 μl acetonitril, and dried completely using a SpeedVac centrifuge. The pieces of gel were reswollen by adding 20 μl of a 10 ng/μl trypsin solution and the samples were incubated overnight at 37 °C. The peptides were extracted by shaking for 20 min with 30 μl of a mixture of 60% acetonitril and 1% trifluoroaceticacid (TFA) in water. The extracted peptides were dried in a SpeedVac centrifuge and dissolved in 10 μl of 0.1% TFA in water. Aliquots of 0.75 μl of the peptide suspension were spotted on the MALDI target and mixed on the target in a 1:1 ratio with the matrix solution consisting of 10 mg/ml α-cyano-4-hydroxycinnamic acid (dissolved in 70% acetonitril and 0.1% TFA). The spots were allowed to dry completely before the MALDI-TOF experiment was performed on the Applied Biosystems 4700 Proteomics Analyzer.

3. Results

3.1. Differential scanning calorimetry of GlcV reveals the presence of a single unfolding transition

Differential scanning calorimetry (DSC) is a powerful technique to study the thermodynamics of protein unfolding and the effects of substrate–enzyme interactions on protein stability. DSC experiments were performed with purified GlcV, the NBD of the glucose transporter of *S. solfataricus*, a hyperthermoacidophile that grows optimal at 85 °C and pH 2.5. Proteins of this organism are highly thermostable and especially suitable for DSC analysis. The DSC profile of wild-type (wt) GlcV showed a single endothermic transition that was followed by aggregation (Fig. 1A). Both the unfolding and precipitation of the protein were irreversible as the transition was lost upon

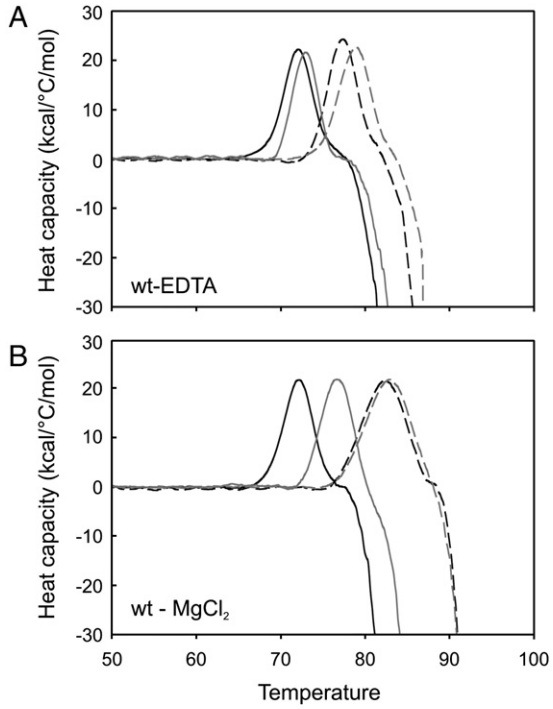

Fig. 1. Differential scanning calorimetry of GlcV. (A) Thermogram of wt GlcV under non-hydrolyzing (2 mM EDTA) and (B) hydrolyzing (5 mM $MgCl_2$) conditions were recorded in the absence of nucleotides (dark line), or in the presence of AMP-PNP (dark grey line), ATP (black long dashed line) or ADP (light grey long dash).

cooling of the sample and subsequent re-scanning (data not shown). The transition midpoint (T_m) for nucleotide-free wt GlcV was 72.0±0.5 °C and remained unchanged in the presence of EDTA) or $MgCl_2$ (Table 1). The observed curve was independent of the scan-rate from 0.5 to 2 °C/min. In an EDTA containing buffer, nucleotide binding resulted in an increase in the T_m compared to nucleotide-free wt GlcV (Fig. 1A). In the presence of ATP or ADP, the increase was about 5.5–6 °C, with a slightly higher up-shift for ADP, while the non-hydrolyzing ATP analogue AMP-PNP caused only a minor up-shift (Table 1). This demonstrated that the nucleotides stabilize the NBD in the order ADP>ATP>AMP-PNP. In the presence of nucleotides, addition of $MgCl_2$ resulted in a further increase of the stability (Fig. 1B). This stabilizing effect was most pronounced in the presence of ATP–Mg^{2+} or ADP–Mg^{2+} yielding similar thermograms with an increase in the T_m of more than 10 °C compared to the nucleotide-free wt GlcV. Again, addition of AMP-PNP–Mg^{2+} caused only a minor up-shift (Table 1). Since addition of Mg^{2+} alone did not increase the stability of the protein, the stabilizing effect of Mg^{2+} seems to occur via interactions with the nucleotide. The unfolding of the nucleotide-free wt GlcV was fitted with a non-two-state model (Table 2). Unfortunately, the data of the nucleotide bound protein could not be fitted since the unfolding was immediately followed by the precipitation of the protein. The fit of the unfolding of nucleotide-free GlcV yielded an enthalpy of unfolding (ΔH_{cal}) and a van't Hoff energy (ΔH_{vH}) of 97 kcal/mol and 222 kcal/mol, respectively. Thus the ratio between ΔH and ΔH_{vH} was close to 0.5 (Table 2). Generally it is assumed

Table 1
Transition temperatures of the thermal unfolding of wt and mutant GlcV in the presence of 2 mM EDTA or 5 mM $MgCl_2$ and various nucleotides

GlcV	T_m (°C)															
	EDTA		$MgCl_2$		ATP+EDTA		ATP+$MgCl_2$		ADP+EDTA		ADP+$MgCl_2$		AMP-PNP+EDTA		AMP-PNP+$MgCl_2$	
wt	72.5		71.8		77.7		82.4		78.5		82.6		72.8		76.4	
G144A	72.8		72.8		76.8		83.0		79.1		83.3		73.9		77.1	
E166A	72.3	77.0	72.2	76.3	77.4	81.2	79.9	83.3	79.7	83.3	79.9	83.3	73.4	77.7	77.3	80.9
E166Q	71.3	75.6	70.6	76.2	79.1	83.2	80.8	83.9	80.2	84.0	80.3	84.0	72.7	77.3	75.7	79.7

The experiments were performed in triplicate and the error in determination of the T_m was less than 0.3 °C.

that the ratio of 0.5 indicates that a protein undergoes structural changes – like dimerization – that change the molar ratio of the active species, though in this experiment, the absence of nucleotides excludes this possibility. The value of 0.5 could also indicate that only part of the protein is unfolded under the conditions employed. As the T_m shows a strong nucleotide dependence, the transition probably corresponds to the unfolding of the NBD while the unfolding of the C-terminal domain does not appear as a separate transition. We propose that the unfolding of the C-terminal domain remains undetected caused by a higher thermostability with a T_m for unfolding above the precipitation temperature. Thus, structurally, GlcV is a two domain protein but by DSC only unfolding of the NBD can be observed.

3.2. GlcV also shows two step unfolding in Guanidiniumchloride

Since the temperature dependent unfolding resulted in aggregation of the protein, we also set out to study the unfolding of GlcV in the presence of the chaotropic reagent Guanidiniumchloride (GndCl). Unfolding was followed using the intrinsic tryptophan fluorescence as a marker. GlcV contains two tryptophans, one located in the NBD and the other located in the C-terminal extension. After incubation of GlcV with increasing concentrations of GdnCl, two distinct unfolding steps could indeed be identified (Fig. 2A–C). The first unfolding step resulted in a decrease of the tryptophan fluorescence (Fig. 2B) with a concomitant red-shift of the fluorescence maximum (Fig. 2C). Surprisingly, this step was followed by a second spectroscopical change which showed an increase in tryptophan fluorescence without a shift of the emission maximum. When similar experiments were performed in the presence of either ATP or ADP, the first unfolding step occurred at higher GndCl concentrations, while the second step, which likely represents further unfolding, was not influenced by addition of ATP or ADP. This confirms that GlcV unfolds in two distinct steps in which first the NBD domain unfolds followed by the unfolding of the C-terminal domain.

Table 2
Thermodynamic parameters of the unfolding of wt and G144A mutant GlcV

GlcV:	ΔH_{cal} (kcal/mol)	ΔH_{vH} (kcal/mol)	$\Delta H_{cal}/\Delta H_{vH}$
wt	97.2±22.5	222±64.0	0.44
G144A	98±14.6	238.3±44.8	0.426

3.3. The G144A mutation does not effect thermal unfolding of GlcV

In the next step, the effects of mutations which block the nucleotide binding domain in a specific step of the ATP hydrolysis cycle were studied. First, a mutation of the second glycine in the ABC signature motif was studied. This mutation does not interfere with nucleotide binding but radically reduces ATP hydrolysis and dimerization in the presence of ATP–Mg^{2+} [13,33]. The DSC profile of G144A GlcV was essentially indistinguishable from that of wt GlcV (data not shown). Again, unfolding occurred with a single endothermic transition both in the presence and absence of nucleotides, at similar transition temperatures as observed for the wt GlcV. In the presence of Mg^{2+}, ADP and ATP both the wt and the G144A GlcV showed similar thermograms. In case of the wt GlcV this is the result of complete hydrolysis of ATP to ADP. The G144A GlcV mutant is radically defective in ATP hydrolysis up to 70 °C, although residual hydrolysis cannot be totally excluded [33]. The long term incubation close to optimal temperature during DSC experiment may trigger a slow ATP hydrolysis by the G144A GlcV. The appearance of similar transition patterns for these two proteins therefore suggests that a similar strong protein–nucleotide interaction occurs that is stabilized by the presence of Mg^{2+} during ATP hydrolysis. The enthalpy of unfolding (ΔH_{cal}) and the van't Hoff energy (ΔH_{vH}) were calculated to be 98 and 238 kcal/mol, respectively. Thus the ratio between ΔH and ΔH_{vH} was again close to 0.5 (Table 2). This indicates that the G144A mutation does not affect the thermal unfolding characteristics of GlcV.

3.4. Thermal unfolding of the E166A GlcV mutant occurs through two transitions

Replacement of the putative catalytic base, *e.g.* the glutamate residue adjacent to the Walker B motif to an alanine results in a strong reduction of the ATPase activity of GlcV. With this mutant, the formation of an ATP dependent stable dimer can be observed by gel filtration [33,34]. Remarkably, DSC of E166A GlcV showed two endothermic transitions under all conditions tested. In the absence of nucleotide, the first T_m (T_{m1}) closely resembled the T_m of the wt and the G144A mutant, whereas the second transition (T_{m2}) occurred at a temperature that is about 4 °C higher. Both transitions were found to be irreversible (data not shown). In the presence of ATP or ADP and EDTA (Fig. 3A), T_{m1} was up-shifted by 5–7 °C and thus essentially comparable to the T_m of the wild-type protein. T_{m2} was also up-shifted but by

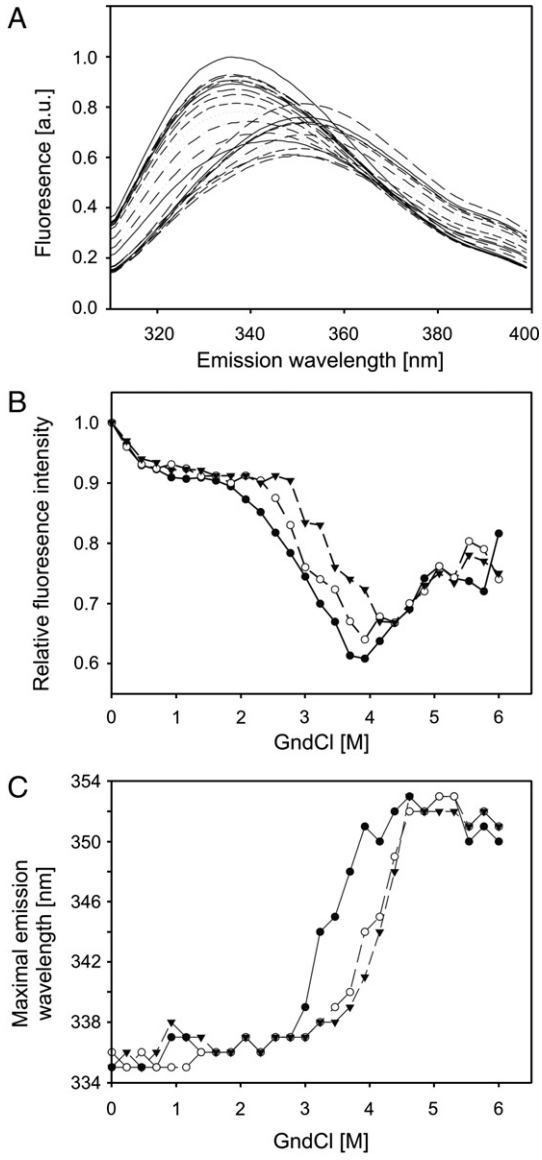

Fig. 2. Unfolding of GlcV in the presence of GndCl. (A) Tryptophan fluorescence spectra (excitation 295 nm, emission 310 to 400 nm) of wt GlcV were determined at increasing GndCl [0–6 M] concentrations. (B) Relative fluorescence intensities and (C) maximum emission wavelengths as a function of the GndCl concentration for wt GlcV in the absence (close circles) of nucleotides, or in the presence of 1 mM ATP (open circles) or ADP (close triangles).

9–11 °C compared to the nucleotide-free wt GlcV (Table 1). The presence of AMP-PNP only slightly influenced the protein stability. The largest increase in T_m was observed in the presence of ATP–Mg^{2+} or ADP–Mg^{2+} (Fig. 3B). Under these conditions, T_{m1} only increased by 7 °C, while the up-shift of T_{m2} was more than 11 °C as compared to the nucleotide-free protein (Table 1). Again, the presence of AMP-PNP–Mg^{2+} induced only a small increase in the T_m values. Since the presence of the two transitions with GlcV E166A was also observed in the nucleotide-free state, this phenomenon cannot be associated with dimerization of GlcV. Therefore, we concluded that the two subdomains which unfold at a similar temperature in wt and G144A GlcV, unfold separately in the E166A mutant. Remarkably, addition of nucleotides results in an up-shift of both T_{m1} and T_{m2} demonstrating that nucleotide binding affects the stability of both subdomains.

To further investigate the structural basis of the two transitions of the GlcV E166A mutant, the previously characterized E166Q mutant [33,34] was also studied by DSC. Whereas substitution of the glutamate by an alanine results in the formation of an empty pocket, substitution by a glutamine only replaces a hydroxyl- by an amino-group. At pH 6.5 at which these experiments are performed, the hydroxyl group most likely is ionized, whereas the amide group of the glutamine does not ionize. As shown previously, mutation of the glutamate to glutamine resulted in an 80% reduction of the ATPase activity of GlcV and the stable formation of the dimer [33,34]. DSC of the nucleotide-free E166Q GlcV mutant again showed two transitions. Importantly, under all conditions tested, the protein showed a dominant first T_m which is at a similar temperature as T_{m1} of the E166A mutant. Remarkably, the observed second transition was much smaller than observed for E166A GlcV (Fig. 3A and B). Addition of ATP or ADP resulted in an up-shift of both T_{m1} and T_{m2} comparable to the shift observed for the E166A mutant. Apparently not only the length of the side chain, but the presence of an acidic group at position 166 strongly affects the structural stability of the subdomain. By changing the carboxyl group of the glutamate to a carboxyamide group, the subdomains of GlcV are apparently stabilized. The glutamate residue has been suggested to play an important role in ATP hydrolysis as a catalytic base [31,42], and in the crystal structure of GlcV, the hydroxyl group interacts with the coordinating water molecule. Apparently this interaction destabilizes the subdomain. It was recently proposed that this glutamate together with the histidine of the H-loop forms a catalytic dyad for ATP hydrolysis. The histidine was suggested to act as a 'linchpin', holding together a complicated network of interactions between ATP, water molecules, Mg^{2+}, and amino acids both in *cis* and *trans*, necessary for intermonomer communication [15]. Possibly mutagenesis of E166 affects this network, and therefore its mutation influences the stability of the ABCα/β and ABCα subdomains.

3.5. Proteolytic cleavage and 8-azido-ATP photoaffinity labelling of wild-type and mutant GlcV proteins

In order to study the domain structure of GlcV in more detail, the enzyme was subjected to proteolytic cleavage by trypsin. GlcV was cleaved into two fragments with apparent sizes of 26 (Frag. 1) and 9 kDa (Frag. 2) on a coomassie stained SDS-PAGE, respectively (see Fig. 5A–C lane 1). To remove uncleaved GlcV, samples were also applied to a gel filtration column. However, both the cleaved and intact GlcV eluted at identical positions, suggesting that the fragments remain associated (data not shown). Analysis of the proteolytic fragments by MALDI-TOF mass spectrometry showed that GlcV was cleaved at lysine residues at positions 83 and 126 resulting in the formation of peptide fragments of 9 and 26 kDa. These positions are indeed exposed in the crystal structure of GlcV (Fig. 4). The remaining mass of 5 kDa could not be

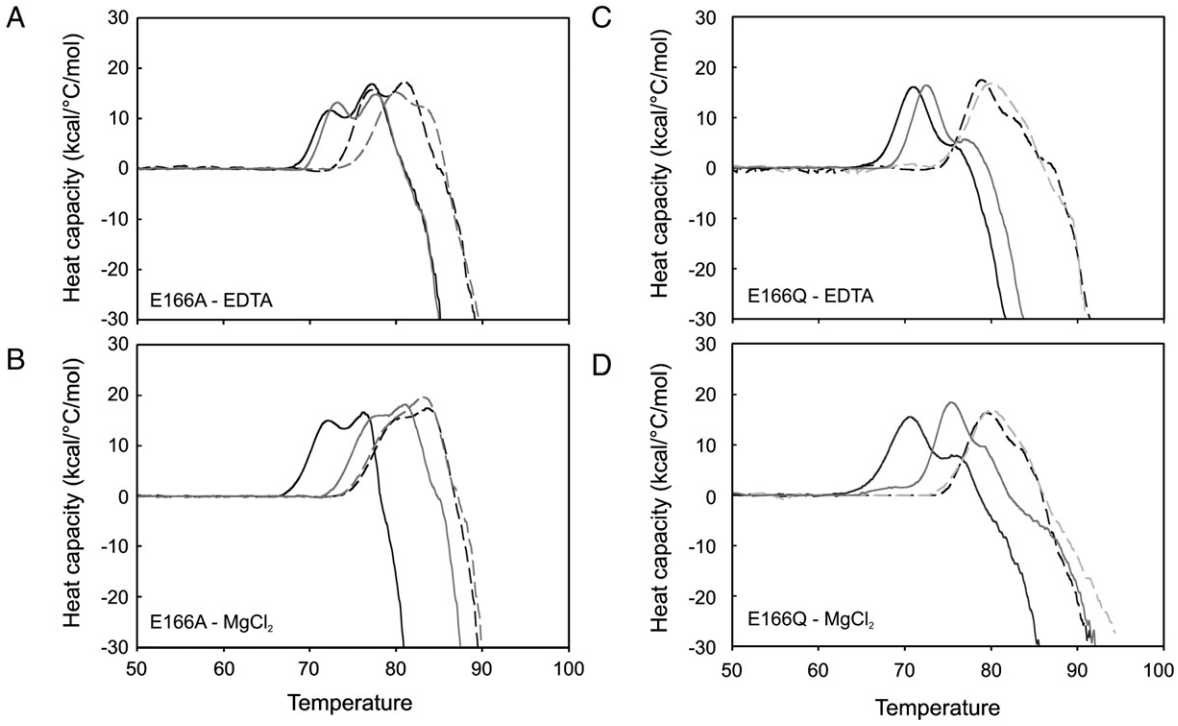

Fig. 3. Differential scanning calorimetry of the G144A, E166A and E166Q mutants GlcV. Thermograms of E166A GlcV (A, B) and E166Q GlcV (C, D) in the presence of 2 mM EDTA (A,C) or 5 mM $MgCl_2$, (B,D) in the absence of nucleotides (dark line), or in the presence of AMP-PNP (dark grey line), ATP (black long dashed line) or ADP (light grey long dash).

detected on SDS-PAGE, but since the corresponding region contains several possible trypsin cleavage sites it is likely further degraded. Cleavage did not occur at the linker region between the N- and C-terminal domains, the NBD (Fig. 4). This is most likely caused by the lack of a trypsin cleavage sites in this region, while the cleavage probability of the site closest to

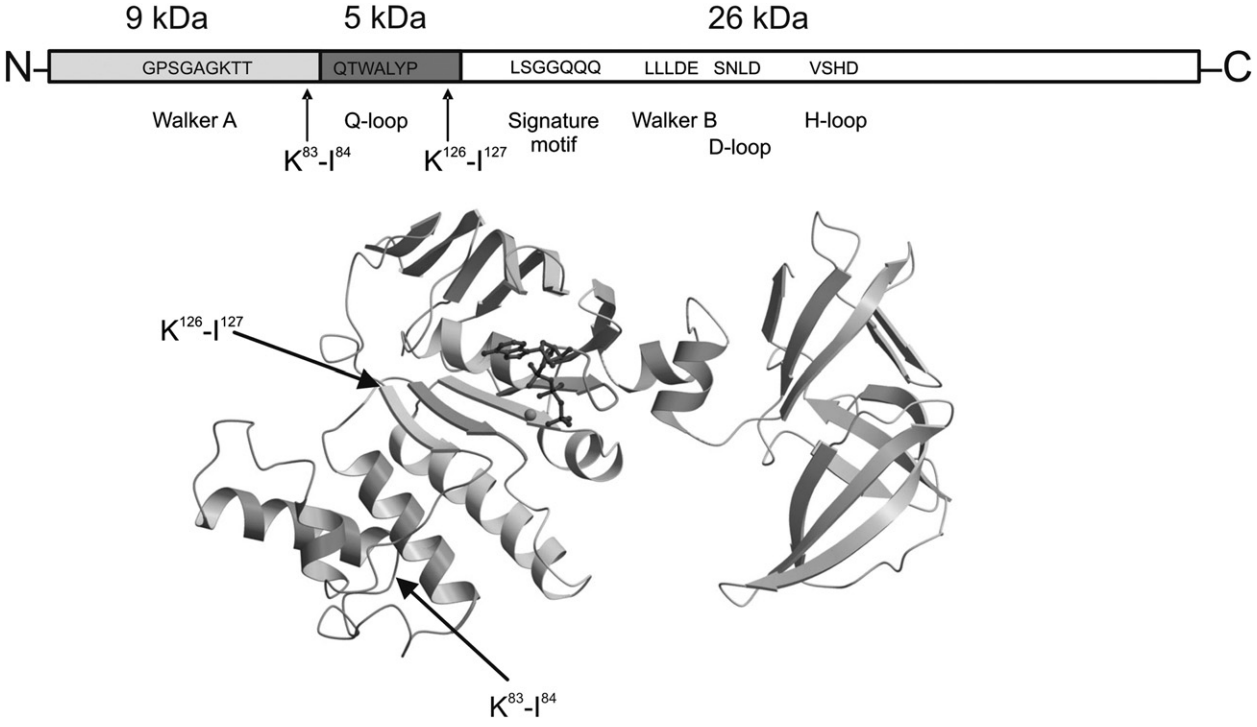

Fig. 4. Sequence alignment of GlcV and the trypsin cleavage fragments identified by mass spectrometry. The light grey area corresponds to the 9 kDa N-terminal fragment, dark grey area indicates a small 5 kDa peptide cleaved by trypsin that is not detected on SDS-PAGE; and the white area corresponds to the 26 kDa cleaved C-terminal peptide. The conserved regions are underlined and indicated below. The arrows in the sequence and GlcV structure (pdb entry: 1OXU) indicate the position of the trypsin cleavage.

the linker region (Lysine 224) is predicted to be negatively influenced by the proline at position 223 [43].

Comparison of the nucleotide-free and nucleotide bound structures of GlcV revealed a re-orientation of the ABCα subdomain and the C-terminal domain relative to the ABCα/β subdomain, and switch-like rearrangements in the P-loop and Q-loop regions [13]. To determine if the tryptic pattern is affected by the nucleotide bound state of the protein, proteolysis was performed in the absence and presence of the different nucleotides for wt GlcV and the G144A and E166A mutants. Remarkably, both the nucleotide-free and ADP–Mg^{2+}-bound wt GlcV exhibited a higher resistance to trypsin digestion than the ATP–Mg^{2+} and AMP-PNP–$Mg2^{+}$ bound forms (Fig. 5). The fragmentation pattern was, however, similar to that of the nucleotide-free wt GlcV. This suggests that a conformational change occurs upon binding of ATP or AMP-PNP but not with ADP. The crystal structures of GlcV in the presence of ADP and AMP-PNP are, however, very similar and only differ in the structure of the Q-loop. In contrast to the nucleotide-free structure, the Q-loop is not disordered in the nucleotide bound structures. The trypsin sensitivity, however, correlates with the observations made with other ABC transporters where ATP binding causes large conformational changes including a rigid body movement of lobe I towards lobe II [11,12]. The overall proteolytic pattern of the two mutants (G144A and E166A) was similar to that of the wt both in the presence and absence nucleotide, except that, the G144A mutant appeared to be more prone to proteolysis. From these data it appears that the ATP dependent dimer formation of the E166A GlcV does not result in an altered proteolysis pattern.

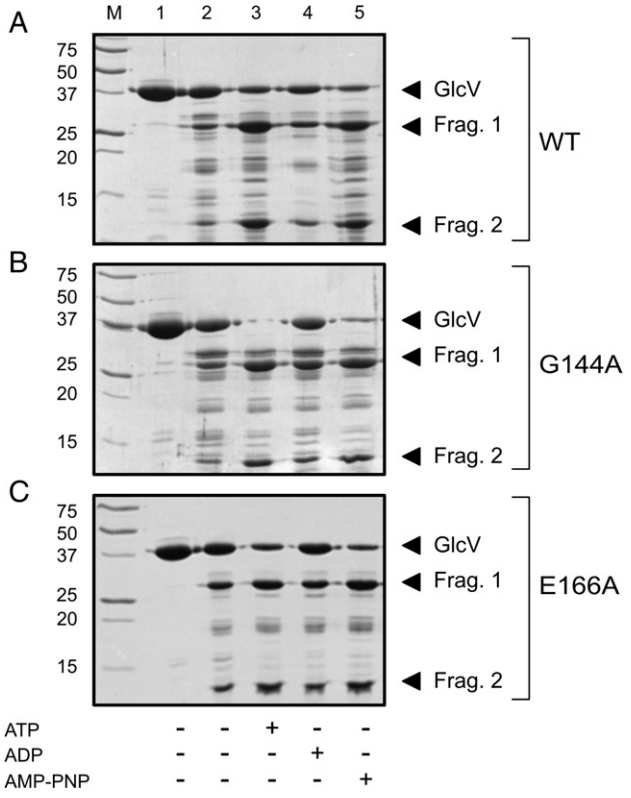

Fig. 5. Nucleotide dependence of trypsin digestion of wt (A), G144A (B) and E166A (C) GlcV. Proteins were digested with trypsin in the presence and absence of different nucleotides. Full length GlcV (lane 1), trypsin digestion in the absence of nucleotide (lane 2), trypsin digestion in the presence of ATP (lane 3), ADP (lane 4) and AMP-PNP (lane 5). The molecular sizes of full length GlcV and cleaved GlcV fragments are indicated by the arrows.

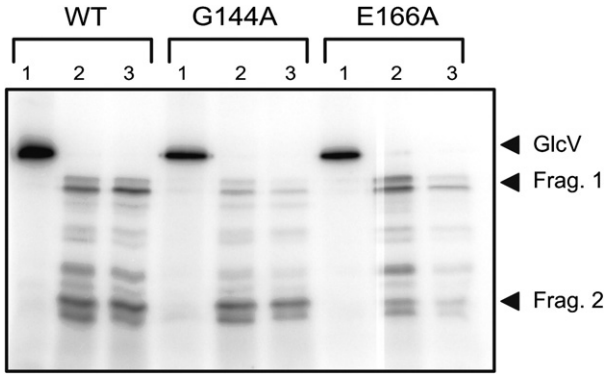

Fig. 6. 8-azido-ATP binding and photocrosslinking of wt, G144A and E166A GlcV. 8-azido-ATP was photocrosslinked to GlcV (lane 1) followed by the digestion of the protein with trypsin (lane 2). In a similar experiment, proteins were first digested with trypsin and subsequently photocrosslinked with 8-azido-ATP (lane 3). Full length and major GlcV fragments are indicated by the arrows.

Next, binding experiments were performed with the photoactivatable nucleotide analogue 8-azido-ATP. Due to the covalent coupling, nucleotide binding to the various proteolytic fragments can be detected. Purified wt and G144A and E166A GlcV showed a similar binding and photocrosslinking to 8-azido-ATP (Fig. 6). After trypsin treatment, nucleotide binding to wt GlcV produced several labelled fragments. The two most dominant fragments are identical to the trypsin digested and mass spectrometry identified fragments described above. The smaller dominant labelled ~9 kDa N-terminal fragment contains the Walker A motif, while the larger ~26 kDa sized C-terminal fragment contains the ABC signature, Walker B motif and the C-terminal domain. 8-azido-ATP binding to the trypsin treated G144A mutant mainly yielded the labelled 9 kDa N-terminal proteolytic fragment, while the E166A mutant showed both prominent 9 and 26 kDa fragments like wt GlcV (Fig. 6). Since the two latter proteins, i.e., wt and the E166A, dimerize upon ATP binding, we conclude that the labelled 26 kDa fragment results from the nucleotide induced dimerization of these proteins. Except for the E166A mutant, isolated GlcV retained the ability to bind nucleotides even after harsh protease treatment.

4. Discussion

Here we have studied the domain organization of an ABC ATPase, GlcV from the hyperthermoacidophile *S. solfataricus* using differential scanning calorimetry and trypsin digestion. GlcV is a subunit of a binding protein-dependent ABC-type glucose transport system. During the ATP hydrolysis cycle, GlcV homodimerizes in an ATP dependent manner. The thermal unfolding of GlcV showed a single transition around 72 °C that was followed by a rapid precipitation of the protein. The midpoint temperature of this transition (T_m) shifted to higher

temperatures in the presence of nucleotides, suggesting a stabilization of the protein. The structure of GlcV, however, indicates a two domain organization, i.e., an N-terminal nucleotide binding domain and a C-terminal domain with unknown function. Nucleotide dependent stabilization and correlation of ΔH to ΔH_{vH} in the absence of nucleotide suggests that the single unfolding event corresponds to the NBD only. The C-terminal domain probably has a higher T_m value but in our experiments this transition point presumably remained undetected due to precipitation of the protein. On the other hand, in the GndCl-induced unfolding, at least two transitions were detectable. The transition at the lower GndCl concentration was stabilized by nucleotides suggesting that this unfolding event corresponds to the NBD. All together our results suggest that wt GlcV and the NBD domain thermally unfold prior to protein precipitation. Moreover, the presence of single thermal transition indicates that the enzyme dimerization is invisible in the DSC thermograms. Previous gel filtration and light scattering experiments [33,34] have indeed shown that wt GlcV is mainly present in the monomeric state, explaining why the dimer is not observed in the DSC experiments.

In addition to the wild-type, we have also investigated the thermal unfolding of several GlcV mutants. These are G144A GlcV with a mutation in the ABC signature motif that does not interfere with nucleotide binding but inactivates the enzyme for nucleotide hydrolysis and dimerization [33,34]; and E166A and E166Q GlcV with mutations of the putative catalytic base adjacent to the Walker B region thereby yielding a protein that still interacts with nucleotide, but that is defective in ATP hydrolysis while retaining the ability to dimerize upon nucleotide binding [33,34]. The thermal unfolding characteristics of the G144A mutant were similar to that of wt GlcV, both in the absence and presence of nucleotides. This demonstrates that the mutation in the ABC signature motif does not lead to structural changes in the GlcV monomer which can be observed using differential scanning calorimetry. In contrast, the E166A and E166Q mutants showed two thermal transitions. The first thermal transition is at a T_m value close to the one observed for wt GlcV and the G144A mutant, while the second T_m was at a temperature 4–5 °C higher. Both T_m values increased in the presence of nucleotide. The presence of the second transition indicates that these mutants have undergone a structural change. Residue E166 has been proposed to act as a catalytic base during ATP hydrolysis [31,42]. In the GlcV structure with bound AMP-PNP, the residue localizes in close vicinity to the γ-phosphate group where it may activate a water molecule for the hydrolytic attack of the β–γ bond of ATP. Mutation of the glutamate to alanine leaves an empty pocket in the structure. It thus appears that the glutamate at this position slightly destabilizes the protein. E166 is located in the ABCα/β subdomain and therefore we hypothesize that the second transition corresponds to unfolding of this subdomain. In the wild-type, the ABCα/β and ABCα subdomains appear to unfold simultaneously. Since the E166A and E166Q mutant both show a second transition, we conclude that the presence of a carboxyl acid group destabilizes the ABCα/β subdomain. This could be a critical feature of the catalytic reaction.

Structural studies on GlcV show that AMP-PNP binds in a similar mode as ADP, except for additional interactions with the three oxygen atoms on the γ-phosphate [13]. Binding of AMP-PNP has been proposed to mimic ATP binding to the monomeric protein. GlcV was found to be more susceptible to proteolysis by trypsin in the presence of ATP or AMP-PNP, while the protein was highly trypsin resistant in the absence of nucleotide or with ADP. Comparison of the ATP, ADP, and nucleotide-free structures of other proteins [11,12,15,17] showed large conformational changes in the Q-loop, and a rigid body movement of lobe I towards lobe II upon binding of ATP. Only minor differences are observed between the ADP-bound and nucleotide-free states. Our trypsin cleavage data is consistent with the conformational changes observed in these structures. Thus, binding of ATP and AMP-PNP to GlcV may induce a movement of lobe I towards lobe II akin to an "induced fit" thereby leading to the formation of the dimerization surface. Interestingly, trypsin cleavage was most pronounced with the monomeric G144A mutant in the presence of ATP or AMP-PNP, while the wt and E166A mutant that both are capable of dimer formation are the most resistant towards trypsin digestion.

Even after harsh protease treatment, GlcV retained the ability to bind 8-azido-[α-^{32}P] ATP, yielding a small labelled ~9 kDa fragment containing the Walker A motif. The Walker A motif interacts directly with the phosphate groups of the bound nucleotide. Our results indicate that only the E166A mutant lost its ability to bind nucleotide after trypsin treatment. Trypsin digestion of the wt and E166A mutant also resulted in the efficient generation of a large labelled 26 kDa fragment which contains the ABC signature motif, Walker B motif and the C-terminal domain. With the G144A mutant, only small amounts of this 26 kDa fragment were obtained. In the monomeric state, the ABC signature motif is located far away from the nucleotide bound lobe I, but it complements the nucleotide binding site in the dimeric state. Therefore, photocrosslinking of 8-azido-ATP under conditions that GlcV dimerizes may result in the labelling of the ABC signature of the C-terminal fragment. Indeed, labelling of the 26 kDa fragment is the strongest with the wild-type and E166A mutant that are both capable of dimerizing. The low level of the 26 kDa fragment with the G144A mutant may thus relate to the monomeric state of this protein. We therefore conclude that the photoaffinity crosslinking approach detects the formation of the dimeric state of GlcV.

The crystal structures of *E. coli* MalK show that the C-terminal domains also forms dimer [17]. The predicted structure of the GlcV dimer also suggests contacts between the two C-terminal domains as they are positioned close to each other while presenting a substantial region to the cytoplasm [13]. Such stable contacts require a rather flexible linker region between the NBD and the C-terminal domain. Attempts to express a truncation of GlcV with only the NBD proved difficult as we could recover the protein only in inclusion bodies (data not shown). Insertion of a thrombin cleavage site in the putative linker domain between the NBD and C-terminal domain resulted in a heat instable protein, while trypsin digestion of GlcV yielded a cleaved NBD rather than the separate NBD and C-terminal domains. It therefore appears that there are

considerable interactions between the two domains which are consistent with the presumed structural role of the C-terminal domain. The DSC data suggest that GlcV thermodynamically behaves as a single domain protein wherein the N- and C-terminal domains may have considerable interaction beside the linker region. The protein shows a strong ability to retain its nucleotide binding and dimerization activities even after harsh protease treatment indicating a rigorous protein structure leading to a functionally highly stable ATPase.

Acknowledgements

This work was supported by the MEMBMACS training network and funded by EU TMR contract HPRN-CT-2000-00075. Chris van der Does and Sonja-Verena Albers were supported by TALENT- and VIDI-grants of the Netherlands Organization for scientific research (NWO).

References

[1] C.F. Higgins, ABC transporters: from microorganisms to man, Annu. Rev. Cell Biol. 8 (67–113) (1992) 67.
[2] A.L. Davidson, J. Chen, ATP-binding cassette transporters in bacteria, Annu. Rev. Biochem. 73 (241–68) (2004) 241.
[3] J.E. Walker, M. Saraste, M.J. Runswick, N.J. Gay, Distantly related sequences in the alpha- and beta-subunits of ATP synthase, myosin, kinases and other ATP-requiring enzymes and a common nucleotide binding fold, EMBO J. 1 (1982) 945.
[4] K.P. Hopfner, A. Karcher, D.S. Shin, L. Craig, L.M. Arthur, J.P. Carney, J.A. Tainer, Structural biology of Rad50 ATPase: ATP-driven conformational control in DNA double-strand break repair and the ABC-ATPase superfamily, Cell 101 (2000) 789.
[5] K.J. Linton, C.F. Higgins, The *Escherichia coli* ATP-binding cassette (ABC) proteins, Mol. Microbiol. 28 (1998) 5.
[6] S.V. Ambudkar, I.W. Kim, D. Xia, Z.E. Sauna, The A-loop, a novel conserved aromatic acid subdomain upstream of the Walker A motif in ABC transporters, is critical for ATP binding, FEBS Lett. 580 (2006) 1049.
[7] G. Schmees, A. Stein, S. Hunke, H. Landmesser, E. Schneider, Functional consequences of mutations in the conserved 'signature sequence' of the ATP-binding-cassette protein MalK, Eur. J. Biochem. 266 (1999) 420.
[8] E. Schneider, S. Hunke, ATP-binding-cassette (ABC) transport systems: functional and structural aspects of the ATP-hydrolyzing subunits/domains, FEMS Microbiol. Rev. 22 (1998) 1.
[9] L.W. Hung, I.X. Wang, K. Nikaido, P.Q. Liu, G.F. Ames, S.H. Kim, Crystal structure of the ATP-binding subunit of an ABC transporter, Nature 396 (1998) 703.
[10] K. Diederichs, J. Diez, G. Greller, C. Muller, J. Breed, C. Schnell, C. Vonrhein, W. Boos, W. Welte, Crystal structure of MalK, the ATPase subunit of the trehalose/maltose ABC transporter of the archaeon *Thermococcus litoralis*, EMBO J. 19 (2000) 5951.
[11] Y.R. Yuan, S. Blecker, O. Martsinkevich, L. Millen, P.J. Thomas, J.F. Hunt, The crystal structure of the MJ0796 ATP-binding cassette. Implications for the structural consequences of ATP hydrolysis in the active site of an ABC transporter, J. Biol. Chem. 276 (2001) 32313.
[12] N. Karpowich, O. Martsinkevich, L. Millen, Y.R. Yuan, P.L. Dai, K. MacVey, P.J. Thomas, J.F. Hunt, Crystal structures of the MJ1267 ATP binding cassette reveal an induced-fit effect at the ATPase active site of an ABC transporter, Structure 9 (2001) 571.
[13] G. Verdon, S.V. Albers, B.W. Dijkstra, A.J. Driessen, A.M. Thunnissen, Crystal structures of the ATPase subunit of the glucose ABC transporter from *Sulfolobus solfataricus*: nucleotide-free and nucleotide-bound conformations, J. Mol. Biol. 330 (2003) 343.
[14] L. Schmitt, H. Benabdelhak, M.A. Blight, I.B. Holland, M.T. Stubbs, Crystal structure of the nucleotide-binding domain of the ABC-transporter haemolysin B: identification of a variable region within ABC helical domains, J. Mol. Biol. 330 (2003) 333.
[15] J. Zaitseva, S. Jenewein, T. Jumpertz, I.B. Holland, L. Schmitt, H662 is the linchpin of ATP hydrolysis in the nucleotide-binding domain of the ABC transporter HlyB, EMBO J. 24 (2005) 1901.
[16] J. Zaitseva, C. Oswald, T. Jumpertz, S. Jenewein, A. Wiedenmann, I.B. Holland, L. Schmitt, A structural analysis of asymmetry required for catalytic activity of an ABC-ATPase domain dimer, EMBO J. 25 (2006) 3432.
[17] J. Chen, G. Lu, J. Lin, A.L. Davidson, F.A. Quiocho, A tweezers-like motion of the ATP-binding cassette dimer in an ABC transport cycle, Mol. Cell 12 (2003) 651.
[18] R. Gaudet, D.C. Wiley, Structure of the ABC ATPase domain of human TAP1, the transporter associated with antigen processing, EMBO J. 20 (2001) 4964.
[19] H.A. Lewis, S.G. Buchanan, S.K. Burley, K. Conners, M. Dickey, M. Dorwart, R. Fowler, X. Gao, W.B. Guggino, W.A. Hendrickson, J.F. Hunt, M.C. Kearins, D. Lorimer, P.C. Maloney, K.W. Post, K.R. Rajashankar, M.E. Rutter, J.M. Sauder, S. Shriver, P.H. Thibodeau, P.J. Thomas, M. Zhang, X. Zhao, S. Emtage, Structure of nucleotide-binding domain 1 of the cystic fibrosis transmembrane conductance regulator, EMBO J. 23 (2004) 282.
[20] F. Scheffel, U. Demmer, E. Warkentin, A. Hulsmann, E. Schneider, U. Ermler, Structure of the ATPase subunit CysA of the putative sulfate ATP-binding cassette (ABC) transporter from *Alicyclobacillus acidocaldarius*, FEBS Lett. 579 (2005) 2953.
[21] R.J. Dawson, K.P. Locher, Structure of a bacterial multidrug ABC transporter, Nature 443 (2006) 180.
[22] K. Hollenstein, D.C. Frei, K.P. Locher, Structure of an ABC transporter in complex with its binding protein, Nature 446 (2007) 213.
[23] R.J. Dawson, K.P. Locher, Structure of the multidrug ABC transporter Sav1866 from *Staphylococcus aureus* in complex with AMP-PNP, FEBS Lett. 581 (2007) 935.
[24] H.W. Pinkett, A.T. Lee, P. Lum, K.P. Locher, D.C. Rees, An inward-facing conformation of a putative metal-chelate-type ABC transporter, Science 19 (315) (2007) 373.
[25] K.P. Locher, A.T. Lee, D.C. Rees, The *E. coli* BtuCD structure: a framework for ABC transporter architecture and mechanism, Science 296 (2002) 1091.
[26] G. Obmolova, C. Ban, P. Hsieh, W. Yang, Crystal structures of mismatch repair protein MutS and its complex with a substrate DNA, Nature 407 (2000) 703.
[27] J. Lowe, S.C. Cordell, E.F. van den, Crystal structure of the SMC head domain: an ABC ATPase with 900 residues antiparallel coiled-coil inserted, J. Mol. Biol. 306 (2001) 25.
[28] A. Karcher, K. Buttner, B. Martens, R.P. Jansen, K.P. Hopfner, X-ray structure of RLI, an essential twin cassette ABC ATPase involved in ribosome biogenesis and HIV capsid assembly, Structure 13 (2005) 649.
[29] E. Schneider, S. Hunke, ATP-binding-cassette (ABC) transport systems: functional and structural aspects of the ATP-hydrolyzing subunits/domains, FEMS Microbiol. Rev. 22 (1998) 1.
[30] P.C. Smith, N. Karpowich, L. Millen, J.E. Moody, J. Rosen, P.J. Thomas, J.F. Hunt, ATP binding to the motor domain from an ABC transporter drives formation of a nucleotide sandwich dimer, Mol. Cell 10 (2002) 139.
[31] J.E. Moody, L. Millen, D. Binns, J.F. Hunt, P.J. Thomas, Cooperative, ATP-dependent association of the nucleotide binding cassettes during the catalytic cycle of ATP-binding cassette transporters, J. Biol. Chem. 277 (2002) 21111.
[32] A. Bohm, J. Diez, K. Diederichs, W. Welte, W. Boos, Structural model of MalK, the ABC subunit of the maltose transporter of *Escherichia coli*: implications for mal gene regulation, inducer exclusion, and subunit assembly, J. Biol. Chem. 277 (2002) 3708.
[33] M.G. Pretz, S.V. Albers, G. Schuurman-Wolters, R. Tampe, A.J. Driessen, D.C. van der, Thermodynamics of the ATPase cycle of GlcV, the nucleotide-binding domain of the glucose ABC transporter of *Sulfolobus solfataricus*, Biochemistry 19 (45) (2006) 15056 (%).
[34] G. Verdon, S.V. Albers, O.N. van, B.W. Dijkstra, A.J. Driessen, A.M. Thunnissen, Formation of the productive ATP–Mg2+-bound dimer of

GlcV, an ABC-ATPase from *Sulfolobus solfataricus*, J. Mol. Biol. 334 (2003) 255.
[35] E. Janas, M. Hofacker, M. Chen, S. Gompf, D.C. van der, R. Tampe, The ATP hydrolysis cycle of the nucleotide-binding domain of the mitochondrial ATP-binding cassette transporter Mdl1p, J. Biol. Chem. 278 (2003) 26862.
[36] C. van der Does, R. Tampe, Changing orders-primary and secondary membrane transporters revised, ChemBioChem 5 (2004) 1171.
[37] C. van der Does, R. Tampe, How do ABC transporters drive transport? Biol. Chem. 385 (2004) 927.
[38] C.F. Higgins, K.J. Linton, The ATP switch model for ABC transporters, Nat. Struct. Mol. Biol. 11 (2004) 918.
[39] R.J. Dawson, K. Hollenstein, K.P. Locher, Uptake or extrusion: crystal structures of full ABC transporters suggest a common mechanism, Mol. Microbiol. 65 (2007) 250.
[40] C.H. Panagiotidis, W. Boos, H.A. Shuman, The ATP-binding cassette subunit of the maltose transporter MalK antagonizes MalT, the activator of the *Escherichia coli* mal regulon, Mol. Microbiol. 30 (1998) 535.
[41] G. Verdon, S.V. Albers, B.W. Dijkstra, A.J. Driessen, A.M. Thunnissen, Purification, crystallization and preliminary X-ray diffraction analysis of an archaeal ABC-ATPase, Acta Crystallogr., D Biol. Crystallogr. 58 (2002) 362.
[42] C. Orelle, O. Dalmas, P. Gros, A. Di Pietro, J.M. Jault, The conserved glutamate residue adjacent to the Walker-B motif is the catalytic base for ATP hydrolysis in the ATP-binding cassette transporter BmrA, J. Biol. Chem. 278 (2003) 47002.
[43] V. Keil-Dlouha, V.N. Zylber, J. Imhoff, N. Tong, B. Keil, Proteolytic activity of pseudotrypsin, FEBS Lett. 16 (1971) 291.